Journal of King Saud University - Science 36 (2024) 103490

HOSTED BY

Contents lists available at ScienceDirect

Journal of King Saud University - Science

journal homepage: www.sciencedirect.com

Full Length Article

Rapid diagnostics for monitoring chronic kidney disease aggravated as a post COVID complication

Priya Paliwal [a,1], Dignya Desai [a,1], Nemat Ali [b], Mohammad Khalid Parvez [c], Mohammad Rizwan Alam [d], Kyung Jin Seo [d,*], Manali Datta [a,*]

[a] Amity Institute of Biotechnology, Amity University, Rajasthan 303007, India
[b] Department of Pharmacology and Toxicology, College of Pharmacy, King Saud University, P.O. Box 2457, Riyadh 11451, Saudi Arabia
[c] Department of Pharmacognosy, College of Pharmacy, King Saud University, P.O. Box 2457, Riyadh 11451, Saudi Arabia
[d] Department of Hospital Pathology, College of Medicine, Uijeongbu St. Mary's Hospital, The Catholic University of Korea, Seoul, Republic of Korea

ARTICLE INFO

Keywords:
COVID-19 complication
Chronic kidney disease
Papain
Cystatin C
Biosensor

ABSTRACT

The prevalence of chronic kidney disease (CKD) is increasing, affecting more than 10 % of the global population. In addition, subclinical inflammation associated with COVID-19 infection leads to a progressive decline in kidney function, resulting in chronic kidney disease. Early intervention in candidates with early-stage CKD may delay, or avert, progression to end-stage complications. It is widely accepted that serum Cystatin C is a reliable and early indicator of CKD. Urinary Cystatin C tends to increase with the progression of kidney malfunctioning. Thus, early detection can lower the morbidity and mortality associated with CKD. This study includes the design of a proteotronic platform for the rapid detection of CKD. Here, we have developed a biosensor that is highly specific to Cystatin C and shows a negligible response to other urinary biomarkers. The sensitivity of the biosensor was 50889.6 μA cm^{-2} mg^{-1} and the limit of detection for Cystatin C in the sample was calculated as 26 ng mL^{-1}. The stability of the biosensor was studied by measuring the change inthe differential pulse voltammetric current at every month of storage at 4 °C. The biosensor was established to be stable for 12 months, with approximately 10 % loss in the preliminary peak current (Ip) value with storage at 4 °C. Thus, the fabricated proteotronic biosensor exhibited an analytical yet simple approach for point of care diagnostics (POCD) of CKD. The developed POCD is economical and proficient, and will enable CKD management in non-hospitalized patients.

1. Introduction

Worldwide Covid-19 has affected more than 680 million people; comorbidities like diabetes, cardiovascular disease, and hypertension have added to the severity of COVID-19, emphasizing the need to curb lifestyle diseases at an early onset. A major post COVID complication is chronic inflammation and minor injuries of the kidney reflected by reduced function leading to advanced kidney failure. COVID-19 infection tends to generate thrombotic clots resulting in occlusion of smaller blood vessels, inducing a slow, yet constant impairment in kidney function (Biswas et al., 2021). Moreover, COVID-19 induces tubular damage via a complement cascade, resulting in infiltration of $CD68^{+}$ macrophages in the interstitial cell of the tubules. Some osmolytes like myo-inositol, sorbitol, glycine betaine, glycerophosphocholine and taurine have been observed to impart integrity to the tubular walls of the kidney yet they are not able to combat the perforations caused by clots (Dar et al., 2017, Hassan et al., 2020). Data indicate that 5 % of COVID survivors demonstrate a 30 % decline in the kidneys' glomerular filtration rate (GFR) (Athari et al., 2020). Chronic kidney disease (CKD) is characterized by progressive deterioration of tubular secretion in the kidneys. The malfunctioning of tubular secretion results in leakage of biomarkers into the urine, which are generally metabolized in a normal functional kidney. Dysbiotic microbial population, obesity, and smoking, in addition to lifestyle diseases such as diabetes, cardiovascular disease, hypertension, and hormone imbalances are key regulators resulting in intensification of symptoms (Lee et al., 2018). Additionally, patients with mild CKD were found to be prone to COVID-19, and vice versa. With long COVID evident in one out of every eight patients (Davis

Peer review under responsibility of King Saud University.

* Corresponding authors.
E-mail addresses: ywacko@catholic.ac.kr (K.J. Seo), mdatta@jpr.amity.edu (M. Datta).

[1] These two authors have contributed equally.

https://doi.org/10.1016/j.jksus.2024.103490
Received 10 June 2024; Received in revised form 17 October 2024; Accepted 19 October 2024
Available online 29 October 2024

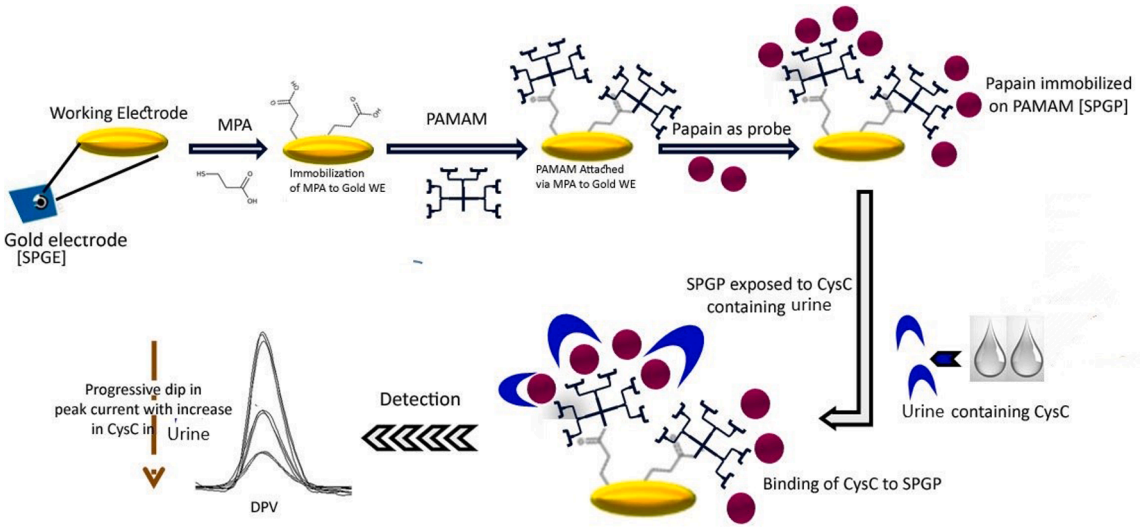

Scheme 1. Schematic outline of a non-invasive proteotronic approach to find the CKD biomarker CysC in human urine. A covalent immobilization of papain as a probe was achieved on the Au/MPA/PAMAM nanohybrid working surface through the application of EDC: NHS chemistry. A 5 mM potassium ferricyanide indicator was used to measure the current generated by SPGP upon incubation with increasing concentrations of CysC for 10 min at room temperature. Probe's (SPGP/papain) electrochemical reaction to CysC was tested using DPV.

et al., 2023), the kidney becomes prone to tubular injury, vascular injury, or podocytopathy (Long et al., 2022). Studies indicated that patients with long COVID predisposed to kidney malfunction suffer from an eGFR loss of −3.26 ml/min/1.73 m^2 annually (Lai et al., 2023). Additionally, CKD itself carries a burden, affecting almost 843.6 million individuals worldwide (Jager et al., 2019). The statistics of CKD has prompted initiatives to develop and implement effective preventative measures aimed at detecting CKD and slowing its progression to ESRD. Detection of CKD is solely based on hospital-based diagnostics; presence of in-vitro diagnostics (IVD) for kidney is almost non-existent (Akben 2018). Early detection followed by prognostic care might prevent the symptomatic progression to end-stage kidney failure.

Currently, several biomarkers have been reported to monitor transition and progression of kidney malfunction. Cystatin C (CysC) is a 13 kD proteinase inhibitor generated by nucleated cells; serum CysC serves as a novel biomarker indicating false-positive decreased GFR. Additionally, CysC is identified as one of the consistent biomarkers present in urine corresponding to tubular impairment of the kidney (Fischer, 2024, Desai et al., 2018). Normal glomerular filtration ensures proper CysC excretion; malfunction in the tubular anatomy, also known as 'shrunken pore system' of the kidney results in a decrease in GFR coinciding with elevated CysC in urine (Qi et al., 2023, Kesson et al., 2020, Marc et al., 2016). A cohort-based study revealed CysC may be used as a measure of kidney dysfunction following COVID-19 and may be used to monitor patients even after they leave the hospital (Gottlieb et al., 2023, Sjöström et al., 2023, Matuszewski et al., 2022). Thus, elevated sCysC measures glomerular damage and COVID-19 severity, whereas uCysC presents itself in tubular injury, acting as a certified biomarker for assessing, grading, and staging of CKD (Lin et al., 2021).

With the current load on the healthcare system and pandemic prevalence, individuals may be reluctant to undergo frequent hospital screenings. Biosensors as a point of care diagnostic tool enable enhanced sensitivity and selectivity with the possibility of rapid data collection without logistic hassles (Azad & Chandra, 2023, Datta et al., 2017, Soveri et al., 2020, Purohit et al., 2019). Availability of a CysC confirmatory test as a point of care diagnostics (POCD) tool may enable substantial monitoring of the recovered COVID-19 candidates with an appropriate resource utilization for patients at increased risk for CKD complications.

In this article, we report a nano-biosensor for CKD stage detection. As a functional control electrode, a dendrimer-modified screen-printed gold electrode (SPGE) immobilized with papain was created. Using differential pulse voltammetry (DPV), the binding affinity of papain to the CKD biomarker CysC (Desai et al., 2018) on the working electrode was determined. When compared to other methods, the label-free electrochemical sensor's advantages in terms of sensitivity, specificity, and limit of detection (LOD) were validated. As a result, a template for creating IVD devices for kidney abnormalities was developed and validated using a non-invasive, quick, inexpensive, and highly sensitive analytical method (Nocek et al., 1996).

2. Experiments

2.1. Materials

Sigma-Aldrich, USA supplied the following: Albumin, Amylase, and Papain, N-hydroxy succinimide (NHS), mercaptopropionic acid (MPA), 1-Ethyl-3-(3-dimethylaminopropyl) carbodiimide (EDC) and poly-amidoamine dendrimer (PAMAM) (fourth generation, MW 14215.0). Thermo Fisher Scientific provided CysC, and Sigma Aldrich provided the. While ethanol and other chemicals were acquired from Qualigens, India, potassium hexacyanoferrate (III) K3[Fe(CN6)] and screen-printed gold electrode (SPGE) were acquired from DropSens and modified in the lab. Every reagent used was of analytical quality, and solutions were made in phosphate buffer (0.01 mM) at pH 7.2.

2.2. Fabrication of functionalized electrode

SPGE was chemically altered to function as a biosensor, with gold working and counter electrodes and silver as the reference electrode. Initially, a stable monolayer was formed by applying 6 µl of 99 % MPA on the working electrode (surface area: 0.126 cm2) for 18 h at room temperature (RT, 27 °C)(Kumar et al., 2020, Lee et al., 2014). After removing extra MPA from the electrode, it was dried at RT. In autoclaved Milli-Q water, an equimolar solution of 10 mM EDC and NHS (1:1 v/v) was incubated for one hour on SPGE (Coates), cleaned, and dried at RT. Next, the working electrode was incubated with 6 µl of PAMAM solution for 3 h. The dendrimers (poly-amidoamine, PAMAM) enable improved loading efficiency of the probe and increase the sensitivity of the designed electrochemical platform (Satija et al., 2011). Through EDC:NHS chemistry, an amide bond is created between the –COOH and $–NH_2$ groups of PAMAM. The electrode was extensively cleaned (three to

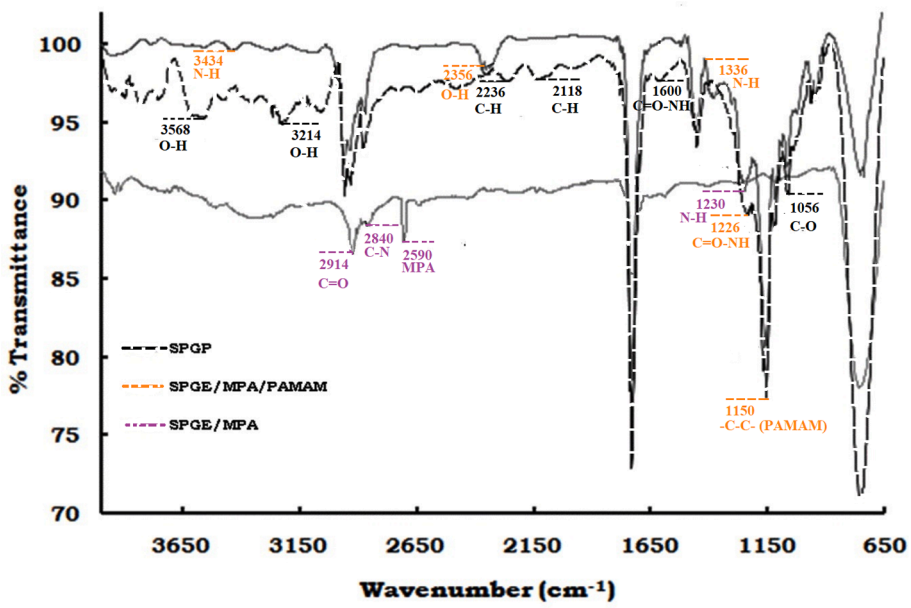

Fig. 1. ATR-FTIR transmission spectra of SPGE/MPA, SPGE/MPA/PAMAM, and SPGE/MPA/PAMAM/Papain from 650–4000 cm^{-1}.

four times) with distilled water in order to get rid of extra PAMAM after bond formation, and it was then dried at room temperature. After loading 6 µl of papain onto the working electrode [SPGP] at room temperature, peptide bonds were formed by the covalent interaction between the papain's –COOH groups and the PAMAM's $–NH_2$ groups. In order to eliminate unbound papain, DW washed three or four times, then dried before electrochemical analysis. Using a NanoDrop spectrophotometer (ND-1000, Thermo Scientific), the amount of unbound papain in the washout was measured at 280 nm.

2.3. Characterization of working electrode (SPGP)

Characterization of surface modification of the working electrode was done by tapping mode atomic force microscopy (AFM, Bruker MultiMode 8, Germany) and Fourier-transform infrared spectroscopy (FTIR, Spectrum-RXI, Perkin Elmer, USA) at 650–4000 cm^{-1}.

2.4. Electrochemical detection of target biomarkers

Using DPV in a 5 mM $K_3[Fe(CN)_6]$ solution as a redox indicator, the electrochemical performance of the electrode was investigated at a 10 mVs^{-1} scan rate and a potential range of −400 mV to 600 mV. Initially, a redox indicator (5 mM $K_3[Fe(CN)_6]$) was used to quantify bare SPGP. Thereafter, SPGP was incubated with different concentrations of CysC (prepared in phosphate buffer) from 100 ng mL^{-1} to 10 mg mL^{-1} for 10 min, followed by washing and drying. DPV for SPGP incubated with different concentrations was monitored using a redox indicator [50 µL]. As the concentration of CysC increased, a steady decline in peak DPV current was noted. Scheme 1 illustrates how Au/MPA/PAMAM is made, how papain is immobilized, and how CysC hybridizes to create SPGP/CysC.

2.5. Sensitivity and selectivity of SPGP

Since albumin and other important proteins are frequently found in urine, a study was done to find the sensor platform's cross-reactivity. Test solutions corresponding to albumin (0.6 mg mL^{-1}) and creatinine (1 mg mL^{-1}) (Govindhan et al., 2014, Soveri et al., 2020) were prepared in phosphate buffer. To achieve this, 6 µl of the biomarkers' test solution was incubated on a fabricated SPGP for 10 min at room temperature (RT), and then it was washed and dried. Following this, in a potential range of −400 mV to 600 mV, electrochemical measurements (Palmsens 4, BaSi, USA) were carried out. Using the previously described method, the selected biomarkers were tested on modified electrodes, and DPV was used to track any changes in current.

Furthermore, SPGP stability was examined by storing at 4 °C for 12 months, with electrochemical measurements (DPV) performed monthly.

3. Results and discussion

3.1. Functionalization of working electrode

Immobilization of papain was conducted using PAMAM, enabling improved loading of the probe and increased sensitivity of the designed electrochemical platform (Lin et al., 2021). Through EDC:NHS chemistry, an amide bond is formed between –COOH groups and $–NH_2$ groups of PAMAM. Quantification of immobilized papain was calculated using a NanoDrop spectrophotometer as described above. In the last step of fabrication, the papain wash solution was collected and analyzed for papain concentration. The NanoDrop-based quantification (280 nm) indicated that approximately 98 µg papain was immobilized on the working electrode.

3.2. Biophysical characterization of SPGP

The attenuated total reflectance-FTIR (ATR-FTIR) spectra was obtained (650–4000 cm^{-1} range) to confirm the surface functional groups of crosslinker, after immobilization of papain and its binding with CysC on a gold screen-printed electrode (Nocek et al., 1996, Datta et al., 2017). The ATR-FTIR transmittance spectra of SPGE/MPA, SPGE/MPA/PAMAM, and SPGE/MPA/PAMAM/Papain electrode are shown in Fig. 1. The significant peaks at 2914 cm^{-1} and 2840 cm^{-1} are explicit for C = O and C-N stretches, respectively. The peak at 2590 cm^{-1} was formed due of MPA molecules onto the gold surface (Lee et al., 2014, López-Cabaña et al., 2015). The spectrum of Au/MPA/PAMAM demonstrated peaks at 1230 cm^{-1} and 1366 cm^{-1} due to N–H bending substituted amide. The peak at 1150 cm^{-1} due to –C–C– bending indicates the presence of PAMAM on the electrode surface (Coates, 2000). The peaks at 2356 and 3434 cm^{-1} are O–H stretching vibrations and N–H stretching, respectively (Satija et al., 2011).

Amide bond formation between PAMAM ($–NH_2$) and papain (–COOH) was determined by peaks at 1600 and 1226 cm^{-1} (Fig. 1)

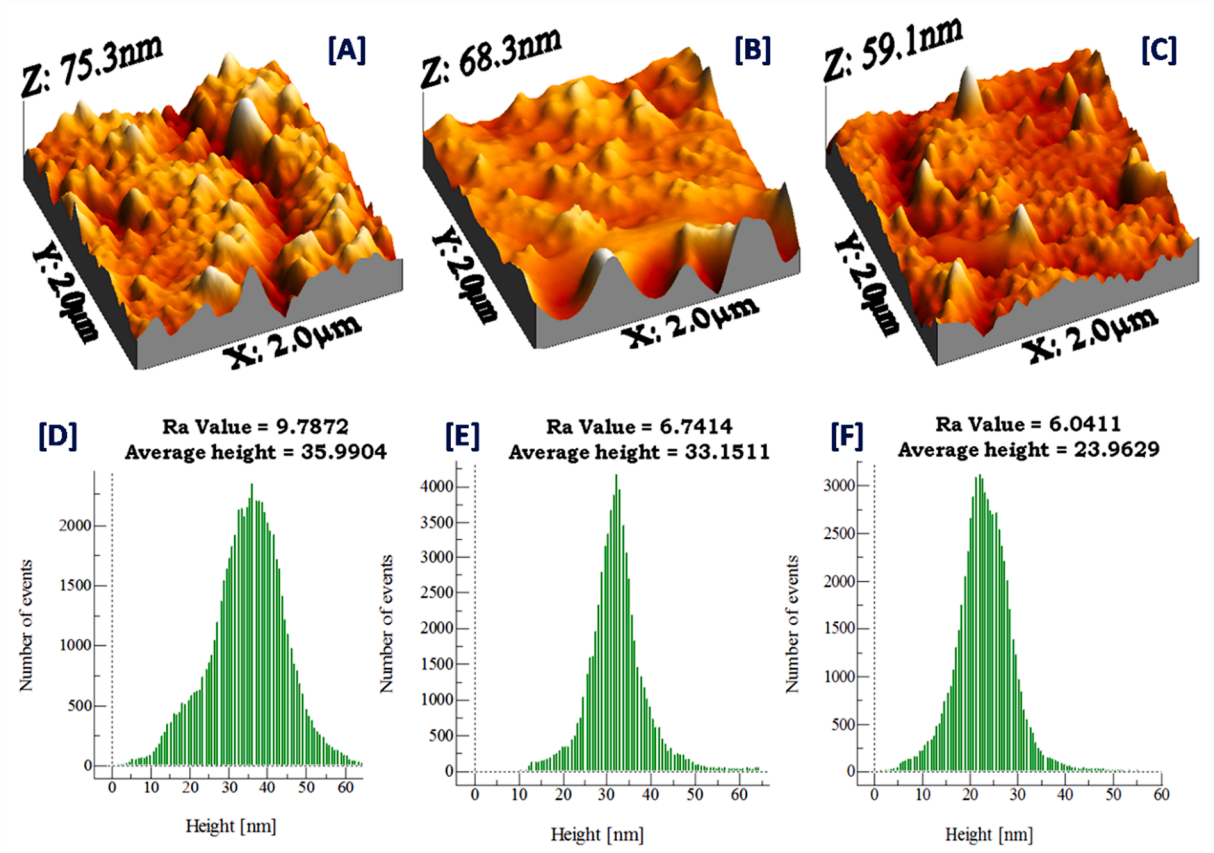

Fig. 2. Surface architecture of SPGE and SPGP. AFM micrographs and distribution of electrode surface thickness: (A & D) Au/PAMAM, (B & E) Au/PAMAM/Papain, (C & F) Au/PAMAM/Papain/CysC. [Data generated by WSxM software].

(Fagerstrom et al., 2015). The peak at 1056 cm^{-1} denotes a C-O stretch, whereas peaks at 2118 cm^{-1}, 2236 cm^{-1}, 3214 cm^{-1}, 3568 cm^{-1}, and 3822 cm^{-1} show C–H and O–H stretching. Papain-CysC binding has already been demonstrated by protein–protein interaction in our previous study (Barth 2007, Skurup et al., 2008).

AFM (Tapping mode) was primarily used to examine the features and roughness factor (Ra) of the surface during consecutive modifications of the electrode. Fig. 2A shows the surface study of Au/PAMAM, with an average Ra value of 9.7873 with 75.3 nm height. Immobilization of papain on the electrode forms an Au/PAMAM/papain complex (Fig. 2 (B)), the surface of which was covered with globular protein molecules with an average Ra value of 6.7414 and height of 68.3 nm. With hybridization of CysC, the surface had 59.1 nm height and 6.0411 Ra value, reflecting the papain-CysC (Fig. 2 (C)) interaction on the modified Au surface (Fischer 2010).

3.3. Electrochemical study of biosensor

With progression in CKD severity, a marked increase in CysC concentration has been established. Assessment of the increase in CKD biomarker was performed using DPV measurements, where the papain-SPGP shows a prominent peak current (Ip) in comparison to the SPGP-CysC. However, the Ip value significantly decreased with increasing CysC concentration. Fig. 3B shows the plot between CysC concentration and relative Ip value; also shown is the hyperbolic curve following the linear equation [Ip (µA) = 3.8072 (µA ng^{-1}) × CysC (ng) + 29.584], with a regression coefficient (R^2) of 0.988. The sensitivity (S) of the biosensor was calculated by the formula (S = m/A), where m was the slope and A was the area of working electrode. The calculated S was 50889.6 µA cm^{-2} mg^{-1} and the LOD, 3(σ/S) for CysC in the sample was calculated as 26 ng mL^{-1} (Fig. 3 A (inset)), and the LOD for CysC in the sample was calculated as 26 ng mL^{-1} (Kaushal et al., 2017). No change was noted in Ip for concentrations corresponding to 15–20 mg mL^{-1}. Using a calibration curve in Fig. 3B and as per the recommendations of International Council for Harmonisation [ICH], LOQ (10σ/S) was calculated to be of 86 ng mL^{-1}.

3.4. Specificity and stability of the sensor

The DPV based specificity of the developed biosensor was tested with different possible biomarkers. The Ip of SPGP at 10 min post incubation with non-specific biomarkers (albumin and creatinine) (Fig. 4 (A)) was weak and decreased after another 10 min (Devasenathipathy et al., 2015, Desai et al., 2018). In contrast, Ip for CysC was consistent after 15 min of incubation, indicating a stable interaction with papain(Bjöerk et al., 1989). As consistency in Ip value was obvious only in CysC, selectivity and specificity of the designed CKD sensor was established.

The stability of the biosensor was monitored monthly based on the changes in DPV current while in storage at 4 °C. It was established to be stable for 12 months based on only 10 % approximate loss in preliminary Ip value during storage at 4 °C [Fig. 4B].

4. Conclusion

A COVID-19-related inflammatory response leads to diffuse proximal tubule damage, which progresses to symptomatic CKD. While detection of CKD is generally serendipitous and is progressive and irreversible, timely detection can postpone complications or requirement of kidney transplant. Patients who suffered from COVID-19 demonstrate pathophysiological mechanisms feed-forwarding the severity of CKD. Assessing the severity of CKD depends on clinical methods, although no bedside diagnostic test is available with timely detection. Due to COVID-

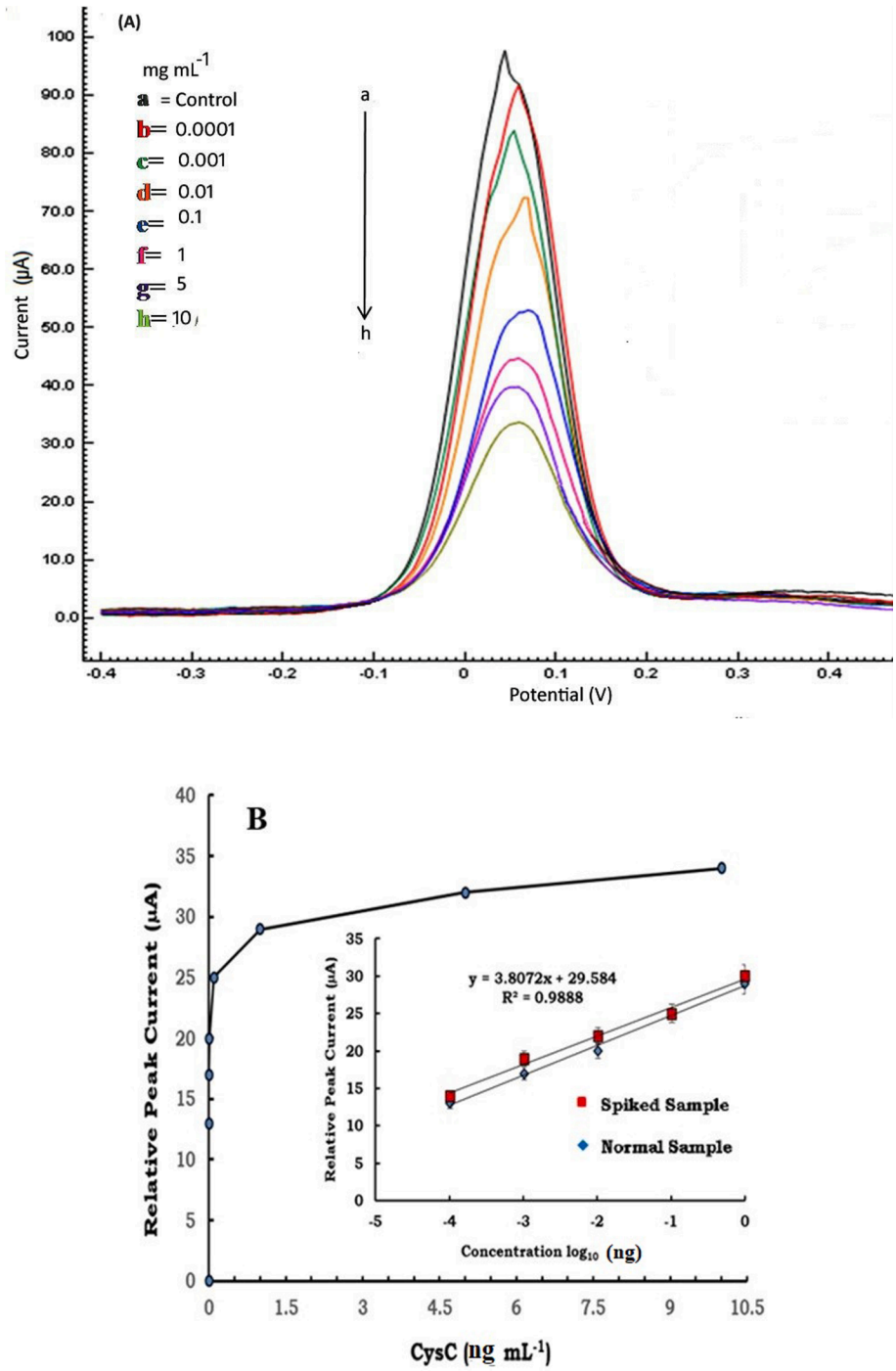

Fig. 3. **(A)** The electrochemical response (DPV) of SPGP was studied using 5 mM $K_3[Fe(CN)_6]$ as a redox reagent. The graph shows DPV of different CysC concentrations from 100 ng mL^{-1} to 10 mg mL^{-1} (b–h). The peak current decreased with increasing concentration of CysC. **(B)** The CysC sensitivity graph, with the CysC concentration in log10 on the Y-axis and relative peak current (μA) on the X-axis. The CysC sensitivity in both normal and spiked samples is displayed in the inset. The Y-axis represents CysC concentration in log10, and the X-axis represents relative peak current (μA). A linear curve for lower concentrations of CysC (0.0001 to 10 mg mL^{-1}) indicates an LOD with an R^2 value of 0.988.

19, patients are hesitant to attend timely checkups, which can add to the disease burden. Nearly the entire global population has been infected with COVID-19 at least once, highlighting the importance of the prognosis of CKD. Bedside diagnostics for CKD may facilitate timely interventions for patients, curbing progression to ESRD.

CysC as a biomarker is more perceptive to sensitive fluctuations during borderline kidney malfunctions and displays better responses as compared to urea or creatinine in kidney impairment in cardiovascular and diabetic patient groups (Zi and Xu, 2018, Stephen et al, 2017). As per kidney disease: Improving Global Outcomes [KDIGO] ranges, urinary CysC range from 0.03 to 0.18 mg/L in normal individuals; whereas levels increase as the severity of kidney failure worsens [4.85 ± 1.29 mg L^{-1} for stage III CKD; 7.39 ± 1.0 mg L^{-1} for stage IV CKD;13.32 ± 1.68 mg L^{-1} for stage V CKD]. CysC is a conventional marker of progressive renal impairment, and association of CysC has been implicated with the inflammatory states of COVID-19 (Zinellu and Mangoni, 2022; Sjostrom et al., 2023).

We demonstrated an ultrasensitive protein–protein interaction-

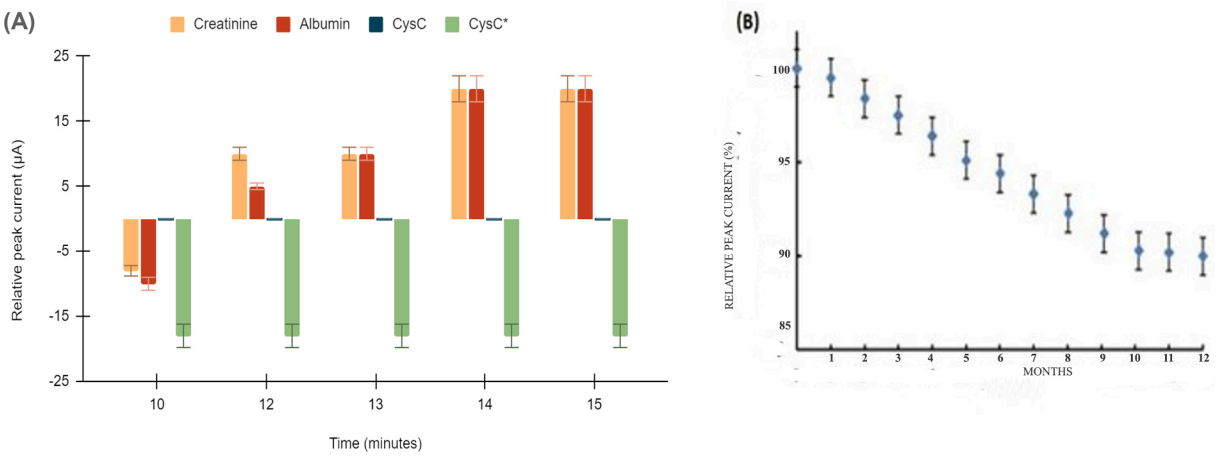

Fig. 4. (A) Specificity of the designed SPGP was evaluated using DPV with CysC, albumin, and creatinine. Two concentrations of CysC were considered: CysC* (highest) (10 mg mL^{-1}) and CysC (lowest) (100 ng mL^{-1}) In comparison to CysC, the other two biomarkers produced negligible signals. **(B)** Stability of the biosensor was measured as % relative Ip every 30 days of stored electrode at 4 °C for a year. Every value is the average of three readings in the same conditions. The Y-axis shows the Ip current of DPV calculated in the range of −400 mV to 600 mV.

Table 1
Comparative table for available CysC kits in market.

TYPE OF DETECTION	DETECTION TIME	PRE-PROCESSING	Range	SENSITIVITY	REFERENCES
ELISA (Rockland)	3 hr	Yes	0.312– 20n g/ml	0.31 ng mL^{-1}	Stephen et al.,2017, Zhang et al., 2024
PETIA (Gentian)	10 min	Yes	0.4—8.0 μg/ml	280 ng mL^{-1}	Stephen et al.,2017
PETIA (Diasys)	10 min	Yes	0.06–1.96 μg/ml	43 ng mL^{-1}	Stephen et al.,2017, Zhang et al., 2024
PENIA (Siemens)	6 min	Yes	0.62–1.11 μg/ml	46 ng mL^{-1}	Kőszegi et al., 2023
Sandwich ELISA (Abcam)	90 min	No	0.312—20 ng/mL	< 10 pg mL^{-1}	Kőszegi et al., 2023
SPGP sensor	10 min	No	100—1 mg/ml	26 ng mL^{-1}	Present

ELISA: Enzyme Linked Immunosorbent Assay; PENIA: Particle Enhanced Nephelometric Assay; PETIA: Particle Enhanced Turbidimetric Assay.

A comparative study was carried out to identify the significance of the fabricated sensor [Table 1]. A previously designed SPRI sensor could detect up to 100 ng mL^{-1} of CysC in serum, which corresponds to the initial stages of kidney deterioration, but will not be able to distinguish from a normal functioning kidney. Additionally, the described method is tedious and not user friendly. Other kits based on enzyme availability are sensitive (Larson et al,2011, but require pre-processing of samples and are not as user friendly as POCT [Table 1]. These tests mentioned have been characterized as qualitative rather than quantitative and may become a hurdle for classification of the CKD stages. Late or failed monitoring of CKD may result in patients incurring heavy burden and reduced quality of life. With the innovative technology presented as a point-of-care solution it is possible to overcome losses arising from kidney malfunction. The developed POCT is economical and proficient, and it will enable CKD management in non-hospitalized patients.

based SPGE platform designed for detection of CysC as a urinary biomarker, a certified biomarker associated with COVID-19-induced CKD. Urine collection as the diagnostic source for CKD detection is painless and causes minimal discomfort to the patient. Hence, using uCysC as a diagnostic source allows comfort and ease as a POCD.

The electrochemical sensor displayed a sensitive response to CysC over a wide linear range of 100 ng mL^{-1} to 1 mg mL^{-1}, with a low detection limit of 26 ng mL^{-1} as projected by DPV. The concentration range corresponds to normal levels of CysC; any progression and persistence of CysC in the urine indicates a deteriorating kidney. Binding of the analyte to the probe was detected within 10 min, which is 30 times shorter than previously reported methods [Table 1] (Bargnoux et al., 2019, Larsson et al., 2011). This ultrasensitive and rapid POCD is capable of detecting the kidney malfunction-specific biomarker CysC with minimal volume (6 μL) and time (10 min) and a limit of quantification (LOQ) of 86 ng mL^{-1} and sensitivity of 50,889.6 μA cm^{-2} mg^{-1} without sample preprocessing. CDC report 2024 cites medicare beneficiaries with CKD had an expenditure of almost $87 billion, whereas for ESKD patients it amounted to almost $115 billion globally. Many CKD initiatives are being implemented for early detection of this progressive degenerative diseases. To date, no diagnostics for CKD are available that can serve as a standalone assessment for kidney degeneration, which may be one of the first prototypes for POCT in the kidney. The average expenditure of an EKSD patient is US$40,000 considering medicare- and hospital-based testing; the availability of this device in the market will lower the cost by 10 times. The technique discussed and validated in this paper has sensitivity, specificity, and enhanced half-life, and requires no trained manpower for handling; thus, the common man can utilize a device developed on this technique from the comfort of his home. Overall, we have achieved our goal of developing a specific and sensitive biosensor for detection of CKD with prolonged shelf life.

CRediT authorship contribution statement

Priya Paliwal: Writing – original draft, Methodology, Investigation, Data curation. **Dignya Desai:** Writing – review & editing, Writing – original draft, Methodology, Formal analysis, Data curation, Conceptualization. **Nemat Ali:** Funding acquisition, Data curation. **Mohammad Khalid Parvez:** Funding acquisition, Data curation. **Mohammad Rizwan Alam:** Writing – review & editing. **Kyung Jin Seo:** Validation, Supervision, Methodology, Investigation, Formal analysis, Conceptualization. **Manali Datta:** Writing – review & editing, Writing – original draft, Validation, Methodology, Investigation, Conceptualization.

Declaration of competing interest

The authors declare that they have no known competing financial interests or personal relationships that could have appeared to influence the work reported in this paper.

Acknowledgments

Authors are thankful to the Researchers Supporting Project Number (RSP2024R379), King Saud University, Riyadh, Saudi Arabia and DST-PURSE grant, SR/PURSE/2021/77, Govt of India for supporting this study. The authors acknowledge North Campus, Delhi University, New Delhi, India, for AFM images.

References

Akben, S.B., 2018. Early-stage chronic kidney disease diagnosis by applying data mining methods to urinalysis.; blood analysis and disease history. IRBM 39 (5), 353–358. https://doi.org/10.1016/j.irbm.2018.09.004.

Athari, S.Z., Mohajeri, D., Nourazar, M.A., Doustar, Y., 2020. Updates on coronavirus (COVID-19) and kidney. J. Nephropathol. 9 (4). https://doi.org/10.34172/jnp.2020.34.

Azad UP, Chandra P. Handbook of Nanobioelectrochemistry. Springer. 2023;1.

Bargnoux, AS., Azoury, V., Badiou, S., Klouche, K., Plawecki, M., Kuster, N., Anne-Marie-Dupuy., Cristol, J.P. 2019. Analytical performances of PENIA and PETIA urinary Cystatin C determination allow tubular injury investigation. Ann. Clin. Biochem. 56 (2), 228-231. Doi: 10.1177/0004563218816341.

Barth, A., 2007. Infrared spectroscopy of proteins. BBA Bioenerg. 1767 (9), 1073–1101. https://doi.org/10.1016/j.bbabio.2007.06.004.

Biswas, S., Thakur, V., Kaur, P., Khan, A., Kulshrestha, S., Kumar, P., 2021. Blood clots in COVID-19 patients: Simplifying the curious mystery. Med. Hypotheses 146, 110371. https://doi.org/10.1016/j.mehy.2020.110371.

Bjoerk, I., Alriksson, E., Ylinenjaervi, K., 1989. Kinetics of binding of chicken cystatin to papain. Biochemistry 28 (4), 1568–1573. https://doi.org/10.1021/bi00430a022.

Coates J. 2000. Interpretation of infrared spectra.; a practical approach.

Dar, M.A., Haque, M.A., Idrees, D., Hassan, M.I., Islam, A., Ahmad, F., 2017. Characterization of folding intermediates during urea-induced denaturation of human carbonic anhydrase II. Int. J. Biol. Macromol. 95, 881–887. https://doi.org/10.1016/j.ijbiomac.2016.10.073.

Datta, M., Desai, D., Kumar, A., 2017. Gene specific DNA sensors for diagnosis of pathogenic infections. Indian J. Microbiol. 57 (2), 139–147. https://doi.org/10.1007/s12088-017-0650-8.

Davis, H.E., McCorkell, L., Vogel, J.M., Topol, E.J., 2023. Long COVID: Major findings.; mechanisms and recommendations. Nat. Rev. Microbiol. 1–14. https://doi.org/10.1038/s41579-022-00846-2.

Desai, D., Kumar, A., Bose, D., Datta, M., 2018. Ultrasensitive sensor for detection of early stage chronic kidney disease in human. Biosens. Bioelectron. 105, 90–94. https://doi.org/10.1016/j.bios.2018.01.031.

Devasenathipathy, R., Mani, V., Chen, S.M., Huang, S.T., Huang, T.T., Lin, C.M., Hwa, K. Y., Chen, T.Y., Chen, B.J., 2015. Glucose biosensor based on glucose oxidase immobilized at gold nanoparticles decorated graphene-carbon nanotubes. Enzyme Microb. Technol. 78, 40–45. https://doi.org/10.1016/j.enzmictec.2015.06.006.

Fagerstrom, P., Sallsten, G., Akerstrom, M., Haraldsson, B., Barregard, L., 2015. Urinary albumin excretion in healthy adults: a cross sectional study of 24-hour versus timed overnight samples and impact of GFR and other personal characteristics. BMC Nephrol. 16 (1), 1–9. https://doi.org/10.1186/1471-2369-16-8.

Fischer, M.J. Amine coupling through EDC/NHS: a practical approach. InSurface plasmon resonance 2010 (pp. 55-73). Humana Press. Doi: 10.1007/978-1-60761-670-2_3.

Fisher, M., Ross, M., DiFranza, L., Reidy, K., 2024. An update on viral infection-associated collapsing glomerulopathy. Adv. Kidney Disease Health 31 (4), 317–325. https://doi.org/10.1053/j.akdh.2023.12.007.

Gottlieb, E.R., Estiverne, C., Tolan, N.V., Melanson, S.E., Mendu, M.L., 2023. Estimated GFR with cystatin C and creatinine in clinical practice: A retrospective cohort study. Kidney Med., 100600 https://doi.org/10.1039/C4RA10399H.

Hassan, M.I., Islam, A., Ahmad, F., 2020. Urea Stress: Myo-inositol's efficacy to counteract destabilization of TIM-β-globin complex by urea is as good as that of the methylamine. Int. J. Biol. Macromol. 151, 1108–1115. https://doi.org/10.1016/j.ijbiomac.2019.10.153.

Jager, K.J., Kovesdy, C., Langham, R., 2019. A single number for advocacy and communication-worldwide more than 850 million individuals have kidney diseases. Kidney Int. 96, 1048–1050. https://doi.org/10.1093/ndt/gfz174.

Kaushal, A., Singh, S., Kumar, A., Kumar, D., 2017. Nano-Au/cMWCNT modified speB gene specific amperometric sensor for rapidly detecting Streptococcus pyogenes causing rheumatic heart disease. Indian J. Microbiol. 57 (1), 121–124. https://doi.org/10.1007/s12088-016-0636-y.

Kesson, A., Lindström, V., Nyman, U., Jonsson, M., Abrahamson, M., Christensson, A., Björk, J., Grubb, A., 2020. Shrunken pore syndrome and mortality: A cohort study of patients with measured GFR and known comorbidities. Scand. J. Clin. Lab. Investig. 80, 412–422. https://doi.org/10.1080/00365513.2020.1759139.

Kőszegi, T., Horváth-Szalai, Z., Ragán, D., Kósa, B., Szirmay, B., Kurdi, C., Mühl, D., 2023. Measurement of urinary Gc-globulin by a fluorescence ELISA technique: Method validation and clinical evaluation in septic patients—A pilot study. Molecules 28 (19), 6864. https://doi.org/10.3390/molecules28196864.

Kumar, A., Purohit, B., Mahato, K., Roy, S., Srivastava, A., Chandra, P., 2020. Design and development of ultrafast sinapic acid sensor based on electrochemically nanotuned gold nanoparticles and solvothermally reduced graphene oxide. Electroanalysis 32 (1), 59–69. https://doi.org/10.1002/elan.201900406.

Lai, S., Gigante, A., Pellicano, C., Mariani, I., Iannazzo, F., Concistrè, A., Muscaritoli, M., 2023. Kidney dysfunction is associated with adverse outcomes in internal medicine COVID-19 hospitalized patients. Eur. Rev. Med. Pharmacol. Sci. 27 (6), 2706–2714. https://doi.org/10.26355/eurrev_202303_31809.

Larsson, A., Hansson, L.O., Flodin, M., Katz, R., Shlipak, M.G., 2011. Calibration of the Siemens cystatin C immunoassay has changed over time. Clin. Chem. 57 (5), 777–778. https://doi.org/10.1373/clinchem.2010.159848.

Lee, H.E., Kang, Y.O., Choi, S.H., 2014. Electrochemical-DNA biosensor development based on a modified carbon electrode with gold nanoparticles for influenza A (H1N1) detection: effect of spacer. Int. J. Electrochem. Sci. 9 (12), 6793–6808. https://doi.org/10.1016/S1452-3981(23)10930-8.

Lee, W.C., Lee, Y.T., Li, L.C., Ng, H.Y., Kuo, W.H., Lin, P.T., Liao, Y.C., Chiou, T.T., Lee, C. T., 2018. The number of comorbidities predicts renal outcomes in patients with stage 3–5 chronic kidney disease. J. Clin. Med. 493 (12). https://doi.org/10.3390/jcm7120493.

Lin, L., Chen, X., Chen, J., Pan, X., Xia, P., Lin, H., Du, H., 2021. The predictive value of serum level of cystatin C for COVID-19 severity. Sci. Rep. 11 (1), 1–8. https://doi.org/10.1038/s41598-021-01570-2.

Long, J.D., Strohbehn, I.A.N., Sawtell, R.A.N.I., Bhattacharyya, R.O.B.Y., Sise, M.E., 2020. COVID-19 Survival and its impact on chronic kidney disease. Transl. Res. 241, 70–82. https://doi.org/10.1016/j.trsl.2021.11.003.

Marc, C., Moutereau, S., Zater, M., Lallali, K., Durrbach, A., Manivet, P., Eschwege, P., Loric, S., 2016. Urinary cystatin C as a specific marker of tubular dysfunction. Clin. Chem. Lab. Med. (CCLM) 44 (2), 288–291. https://doi.org/10.1515/CCLM.2006.050.

Matuszewski, M., Reznikov, Y., Pruc, M., Peacock, FW., Navolokina, A., Júarez-Vela, R., Jankowsk,i L., Rafique, Z., Szarpak, L. 2022. Prognostic Performance of Cystatin C in COVID-19: A Systematic Review and Meta-Analysis. Int J Environ Res Public Health 19(21):14607. Doi: 10.3390/ijerph192114607.

Purohit, B., Mahato, K., Kumar, A., Chandra, P., 2019. Sputtering enhanced peroxidase like activity of a dendritic nanochip for amperometric determination of hydrogen peroxide in blood samples. Microchim. Acta 186, 1–10.

Qi, Z., Yuan, S., Wei, J., Xia, S., Huang, Y., Chen, X., Zhu, X., 2023. Clinical and pathological features of omicron variant of SARS-CoV-2-associated kidney injury. J. Med. Virol. 95 (10). https://doi.org/10.1002/jmv.29196.

Satija, J., Sai, V.V., Mukherji, S., 2011. Dendrimers in biosensors: Concept and applications. J. Mater. Chem. 21 (38), 14367–14386. https://doi.org/10.1039/C1JM10527B.

Sjöström, A., Markgren, P.O., Hansson, M., 2023. Prognostic potential of creatinine and Cystatin C in COVID-19–a retrospective cohort study from Karolinska University Hospital. Scand. J. Clin. Lab. Invest. 83 (4), 251–257. https://doi.org/10.1080/00365513.2023.2210291.

Skurup, A., Kristensen, T., Wennecke, G., 2008. New creatinine sensor for point-of-care testing of creatinine meets the National Kidney Disease Education Program guidelines. Clin. Chem. Lab. Med. 46 (1), 3–8. https://doi.org/10.1515/cclm.2008.004.

Soveri, I., Helmersson-Karlqvist, J., Fellström, B., Larsson, A., 2020. Day-to-day variation of the kidney proximal tubular injury markers urinary cystatin C.; KIM1.; and NGAL in patients with chronic kidney disease. Ren. Fail. 42 (1), 400–404. https://doi.org/10.1080/0886022X.2020.1757463.

Stephen, B.J., Desai, D.I., Datta, M.A., 2017. An alternative diagnostic design for chronic kidney disease detection based on cystatin-c. Asian J. Pharm. Clin. Res. 10, 425–429.

Zhang, L., Nizhamuding, X., Zheng, H., Zeng, J., Yuan, X., Ma, Z., Zhang, C., 2024. An LC–MS/MS method for serum cystatin C quantification and its comparison with two commercial immunoassays. Clin. Chem. Lab. Med. (CCLM) 62 (6), 1092–1100. https://doi.org/10.1515/cclm-2023-0821.

Zinellu, A., Mangoni, A.A., 2022. Cystatin C, COVID-19 severity and mortality: A systematic review and meta-analysis. J. Nephrol. 35 (1), 59–68. https://doi.org/10.1007/s40620-021-01139-2.